CLASSIFICATION CHANGED TO
RESTRICTED
SECURITY INFORMATION
Authority Dryden No. 618 Date
By T. WOODARD See
JAN 16 1952

CONFIDENTIAL

FILE COPY
NO 4

Copy No. 310
RM No. L7D22

CLASSIFICATION CANCELLED
JUL 3 1951

NACA

RESEARCH MEMORANDUM

CLASSIFICATION CANCELLED
BY AUTHORITY J. W. CROWLEY
CHANGE #1581 DATE 12-1-53 T.C.F.

SOME PRESSURE-DISTRIBUTION MEASUREMENTS ON A SWEPT WING AT TRANSONIC SPEEDS BY THE NACA WING-FLOW METHOD

By

J. Ford Johnston and Edward C. B. Danforth

Langley Memorial Aeronautical Laboratory
Langley Field, Va.

LOANED ON LOAN FROM THE FILES OF
NATIONAL ADVISORY COMMITTEE FOR AERONAUTICS
LANGLEY AERONAUTICAL LABORATORY
LANGLEY FIELD, HAMPTON, VIRGINIA
RETURN TO THE ABOVE ADDRESS.
REQUESTS FOR PUBLICATIONS SHOULD BE ADDRESSED AS FOLLOWS:
NATIONAL ADVISORY COMMITTEE FOR AERONAUTICS
1512 H STREET, N. W.
WASHINGTON 25, D. C.

CLASSIFIED DOCUMENT
This document contains classified information affecting the National Defense of the United States within the meaning of the Espionage Act, USC 50:31 and 32. Its transmission or the revelation of its contents in any manner to an unauthorized person is prohibited by law. Information so classified may be imparted only to persons in the military and naval services of the United States, appropriate civilian officers and employees of the Federal Government who have a legitimate interest therein, and to United States citizens of known loyalty and discretion who of necessity must be informed thereof.

NATIONAL ADVISORY COMMITTEE FOR AERONAUTICS
WASHINGTON
June 6, 1947

RESTRICTED
SECURITY INFORMATION

CLASSIFICATION CANCELLED

CONFIDENTIAL

RESTRICTED
SECURITY INFORMATION

NATIONAL ADVISORY COMMITTEE FOR AERONAUTICS

RESEARCH MEMORANDUM

SOME PRESSURE-DISTRIBUTION MEASUREMENTS ON A SWEPT WING AT TRANSONIC SPEEDS BY THE NACA WING-FLOW METHOD

By J. Ford Johnston and Edward C. B. Danforth

SUMMARY

First results are given of chordwise pressure-distribution measurements on a 45° swept-back wing at transonic speeds. These tests are part of a fundamental investigation of flow phenomena near sonic velocity by the NACA wing-flow method. Distributions were obtained at two spanwise extensions of the half-span model of 2-inch chord and NACA 65-210 airfoil section measured perpendicular to the leading edge. These extensions placed the plane of the orifices at 18 percent and 87 percent of the streamwise chord from the plane of symmetry. The corresponding aspect ratios were 2.1 and 3.5, respectively.

The results indicate that:

1. The section at 18 percent chord from the root experienced relatively large changes in the pressure distribution as the Mach number increased to and beyond 1.0; these changes were toward more positive pressures on the forward part of the airfoil and more negative on the rear, accompanied by a rearward shift of the peak negative pressure.

2. The section at 87 percent chord from the root showed relatively small changes in distribution with Mach number up to 1.05 at zero lift and large changes toward more positive pressures on the forward upper surface under lifting conditions at sonic speeds.

3. For both sections, the changes in pressure distribution with Mach number did not indicate any appreciable net loss in the section lift but did indicate large increases in the section drag and diving moment, with the exception of the outboard station at zero lift.

4. The pressure changes at zero lift were in qualitative agreement with those theoretically predicted at sections similarly located with respect to the Mach cones from the root leading and trailing edges.

5. Above a Mach number of 1.0, the region of high drag due to the root extends farther outboard under lifting conditions than at zero lift.

INTRODUCTION

The beneficial effect of wing sweepback in reducing the changes in drag and lift associated with transonic flight speeds has been amply demonstrated as, for example, in references 1 to 3. Comparison of the results with the simple theory for an infinite yawed wing shows, however, that the benefits obtained are considerably smaller than the theoretical. Failure to reach the theoretical results is usually ascribed to disturbances from the root, but no experimental investigations of these flow phenomena through the transonic range have been made previously. Jones has investigated, theoretically, the effects of finite aspect ratio on a nonlifting swept wing in supersonic flow (reference 4). For this case, it is indicated that disturbances from the root cause a high drag inboard and that the tip disturbances may be beneficial. The theory has been applied in reference 5 to study of design parameters for nonlifting swept-back wings.

In order to determine experimentally the flow phenomena on swept wings at transonic speeds, a program of pressure measurements by the NACA wing-flow method has been set up. The first model, like that of reference 1, is an untapered 45° swept-back airfoil with NACA 65-210 2-inch chord sections measured perpendicular to the leading edge.

The small model size limits the number of orifices and makes it difficult to obtain pressures near the leading and trailing edges without errors due to lag. Because of this fact, data so far obtained cover pressure distributions back only to about 77 percent chord for sections near root and midspan for aspect ratios 2.1 and 3.5, respectively. Greater chordwise coverage is to be obtained; in the interim, however, it is felt that the results of these first tests of swept-back-airfoil pressure distributions through the speed of sound are of sufficient interest to justify reporting at this time.

APPARATUS AND PROCEDURE

The airfoil (fig. 1) was mounted to extend into the high-speed air stream over a specially faired ammunition compartment cover on the wing of a P-51D airplane, as shown in figure 2. The curvature of this cover plate was selected to give small horizontal velocity gradients at the model position up to test Mach numbers of about 1.05. Typical gradients and test Reynolds' numbers are given in figure 3. Perpendicular to the cover plate the velocity decreased less than 1 percent per inch. The flow angles and velocities at the model position were calibrated as in reference 1.

A sketch of the 45° swept-back model and its mounting on an end plate flush with the airplane wing surface is given in figure 4. The gap between the airfoil and end plate was sealed to prevent leakage. The airfoil sections perpendicular to the leading edge were of NACA 65-210 profile and 2-inch chord. The tip was cut off parallel to the air stream and slightly rounded. Pressure distributions reported herein were obtained from upper- and lower-surface orifices in a plane parallel to and $2\frac{1}{2}$ inches inboard of the tip. As the airfoil was tested at extensions giving 5-inch and 3-inch semispans, the test section was at 50 percent semispan, aspect ratio 3.5, and 18 percent semispan, aspect ratio 2.1, respectively. In terms of the chord parallel to the stream, these stations were at 0.87 and 0.18 chord from the plane of symmetry. The wing boundary-layer thickness at the model position was of the order of 0.1 inch, or 0.035 model chord. The effects of a boundary layer at the root of a swept wing have not been evaluated. Therefore the inboard position of the orifice plane was taken as not closer than one-half inch (0.18 chord) to the root in an attempt to avoid large boundary-layer effects.

Tests were generally made with seven orifices on the upper and seven orifices on the lower surface to make sure of having upper- and lower-surface distributions at the same angle of attack. The orifice locations are shown in figure 4. In order to check the fairing of the distributions, flights were also made with all orifices on one surface.

Each test was made by diving the airplane from 28,000 feet altitude at a 25° angle, until an airplane Mach number of 0.72 was obtained. This procedure gave Mach numbers at the model station from 0.7 to 1.1. Continuous records on standard NACA recording instruments were taken during the dive of model airfoil pressures and angle of attack, airplane impact pressure and normal acceleration,

and altitude pressure and temperature. The model angle was varied by a motor-driven cam which produced angles of attack by 2° steps from -2° to 4° during test. By this means each of the intermediate angles was obtained about eight times during a dive, and the end angles, -2° and 4°, were obtained about four times.

SYMBOLS

M	stream Mach number
M_N	normal Mach number, $M \cos \Lambda$
q	stream dynamic pressure
q_N	$q \cos^2 \Lambda$
Λ	sweep angle
α	angle of attack in stream direction
α_N	normal angle of attack, $\alpha/\cos \Lambda$ for small angles
c_l	section lift coefficient
c_{l_N}	normal section lift coefficient, $c_l/\cos^2 \Lambda$
$\left(\frac{dC_L}{d\alpha}\right)$	wing lift-curve slope, assumed equal to $\frac{2\pi A}{A + 2} \cos \Lambda$ at $M = 0$
$\left(\frac{dC_L}{d\alpha}\right)_N$	normal lift-curve slope, assumed equal to $\frac{2\pi A}{A + 2}$ at $M = 0$
A	aspect ratio, b^2/S
b	wing span perpendicular to stream direction
S	wing area
c_o	root chord, measured in stream direction
y	spanwise distance from root

RESULTS AND DISCUSSION

From the faired curves of the pressure at each orifice as a function of Mach number and angle of attack, points were taken off at angles of -2°, 0°, 2°, and 4° and at calibrated Mach numbers corrected for vertical gradients of 0.80, 0.90, 1.00, and 1.05. The pressure distributions so obtained are shown in figures 5 and 6. A striking feature of these plots is the almost complete disappearance of negative pressure peaks at the nose as the Mach number approaches 1.0. At the same time, there is an increase in the negative pressures near midchord. For the section near the root, there is also a pronounced rearward movement of the position of maximum suction on both surfaces.

These effects may be studied more conveniently in figures 7 and 8 for angles of -2° for zero lift and of 4° for a lifting condition. The simplest case is that of zero lift, figure 7. Here the effects of the differences in aspect ratio for the two sets of pressure measurements are small and the principal effects are those of Mach number and distance from the root. It may be seen from figure 7 that the sections differ considerably in pressure distribution even at $M = 0.8$ and that the midspan station $y = 0.87c_o$ shows relatively small Mach number effects as compared with the station near the root. At midspan, increasing Mach number beyond 0.9 results in slightly more positive pressures near the nose and more negative pressures near midchord on both upper and lower surfaces, but the peak negative pressure does not move behind maximum thickness up to $M = 1.05$. The section near the root is characterized by relatively larger increases in positive pressure ahead of maximum thickness and pronounced rearward shifts of the peak negative pressure as the Mach number reaches 1.0.

For the lifting condition (fig. 8) the two sections cannot be compared directly at the same angle of attack because of the difference in aspect ratio. The principal feature is the disappearance of the negative peaks at the noses of both sections with increasing Mach number. The change is relatively continuous from $M = 0.8$ for the section near the root, but takes place between $M = 0.9$ and $M = 1.0$ for the midspan station. Again it may be noted that the peak negative pressure at midspan does not move beyond maximum thickness, whereas there is a pronounced rearward shift beyond the midchord for the section near the root. The large changes of the upper-surface pressures near the nose as compared with the lower surface indicate a shift of the stagnation point toward the upper surface with increasing Mach number. This shift tended to reduce the pressure changes with Mach number on the lower surface.

The changes in pressure distribution with Mach number may be interpreted qualitatively as force changes. For example, the increasing positive forward pressures and the rearward movement of the peak negative pressures for the section near the root indicate relatively large increases in drag both at zero lift and under lifting conditions. The midspan section, on the other hand, shows only small changes at zero lift but relatively large drag increases as the Mach number reaches 1.0 under lifting conditions. The fact that the peak negative pressure does not shift beyond midchord indicates that the more outboard station probably has less drag than the other even under lifting conditions.

The center of lift is seen from figure 8 to shift rearward with increasing Mach number for both stations, which indicates an increasing diving moment. The lift itself does not appear to be affected radically, as the loss of lift forward seems to be approximately balanced by gains toward the rear.

It is of interest to compare these pressure distributions with theoretical and experimental distributions on straight wings of the same section and Mach number normal to the leading edge. The theoretical distributions may be obtained from reference 6. Data have been obtained from the Ames 16-foot high-speed wind tunnel for an unswept wing of NACA 65-210 sections, aspect ratio 9.0, and taper ratio 2.5. These data are compared with the theoretical solution given in figures 9 and 10 for zero and positive lift. As the distributions are a function primarily of the lift coefficient, the comparisons are made at the same low-speed normal lift coefficients as computed using the angles from zero lift and the assumed lift-curve slopes (see "Symbols"). The theoretical pressure coefficients have been increased by the Prandtl-Glauert factor for the appropriate normal Mach number.

The distributions of figures 9 and 10 indicate that the pressures at the midspan station $y = 0.87c_o$ may be predicted from the simple theory for both zero and moderate lift coefficients so long as the stream Mach number is subsonic. At a stream Mach number of 1.05, the prediction is still fair for zero lift but unusable for the lifting condition. It is to be noted in particular that the breakdown with lift at the supersonic stream Mach number is not due to the supercritical normal Mach number, since the experimental straight-wing distribution has no similar breakdown.

For the inboard section $y = 0.18c_o$ the similarity to the straight-wing distributions decreases with increasing lift and disappears at the higher Mach numbers. From figures 7 and 8, the deterioration progresses with Mach number from 0.8 up.

The data so far presented show that the simple theory of the infinite yawed wing tends to break down at the root of a finite swept wing. This area of disturbance and drag spreads outboard at transonic speeds, particularly under lifting conditions. More accurate theoretical treatments of the swept wing have been made for the subsonic lifting case by the lifting-surface method, reference 7, and for the supersonic case at zero lift in references 4 and 5. No treatment is yet available for the supersonic lifting condition where the wing is swept back behind the Mach cone. Although a detailed discussion of these theories is beyond the scope of this paper, certain features are of interest.

First, examination of the distribution of circulation on a 30° swept wing in incompressible flow (fig. 1 of reference 7) reveals that the circulation distribution at the center is shifted relatively rearward. By extension, there may be expected a rearward movement of the center of pressure as well as a probable reduction of the negative pressures on the nose in relation to those at midspan. This difference is of the type found in the present tests.

For the supersonic case at zero lift, reference 4 shows that the distribution at the root is of the Ackeret supersonic type, but reduced by the obliquity, and that the distributions change rapidly toward the subsonic type as a function of the section distance behind the root leading-edge Mach cone. The distribution is substantially of the subsonic type when the root leading-edge Mach cone is 1-chord length ahead of the leading edge. At $M = 1.05$ (fig. 9(b)) the Mach cone is about 60 percent chord ahead of the midspan-section leading edge, and as predicted, the distribution at zero lift is very nearly like the subsonic. The differences are in the direction theoretically indicated - toward more positive pressures near the leading edge, followed by a slight overexpansion back to the intersection with the Mach cone from the root trailing edge at 40 or 50 percent chord, then a continuous pressure recovery back to the trailing edge. The inboard section, as predicted, has even more positive pressures on the forward surfaces and pronounced overexpansion behind maximum thickness. As the survey extended only to 77 percent chord, the sharp pressure recovery predicted at 85 percent chord could not be checked experimentally.

The supersonic lifting case introduces a new problem of the effect of the pressure difference between upper and lower surfaces on the inclination of the flow ahead of the wing. The need for a theoretical treatment of this case is pointed out by the large wing area over which these tests show the simple theory to be inadequate.

CONCLUSIONS

Chordwise pressure-distribution tests at two spanwise stations on a swept-back wing model at transonic speeds indicated that:

1. The section at 18 percent chord from the root experienced relatively large changes in the pressure distribution as the Mach number increased to and beyond 1.0; these changes were toward more positive pressures on the forward part of the airfoil and more negative on the rear, accompanied by a rearward shift of the peak negative pressure.

2. The section at 87 percent chord from the root showed relatively small changes in distribution with Mach number up to 1.05 at zero lift but large changes toward more positive pressures on the forward upper surface under lifting conditions at sonic speeds.

3. For both sections the changes in pressure distribution with Mach number did not indicate any appreciable net loss in the section lift, but did indicate large increases in the section drag and diving moment, with the exception noted of the outboard station at zero lift.

4. The pressure changes at zero lift were in qualitative agreement with those theoretically predicted at sections similarly located with respect to the Mach cones from the root leading and trailing edges.

5. Above a Mach number of 1.0, the region of high drag due to the root extends farther outboard under lifting conditions than at zero lift.

Langley Memorial Aeronautical Laboratory
National Advisory Committee for Aeronautics
Langley Field, Va.

REFERENCES

1. Zalovcik, John A., and Adams, Richard E.: Preliminary Tests at Transonic Speeds of a Model of a Constant-Chord Wing with a Sweepback of 45° and an NACA $65_{(112)}$-210, a = 1.0 Airfoil Section. NACA ACR No. L5J16a, 1945.

2. Mathews, Charles W., and Thompson, Jim Rogers: Comparative Drag Measurements at Transonic Speeds of Rectangular and Swept-Back NACA 65_1-009 Airfoils Mounted on a Freely Falling Body. NACA ACR No. L5G30, 1945.

3. Whitcomb, Richard T.: An Investigation of the Effects of Sweep on the Characteristics of a High-Aspect-Ratio Wing in the Langley 8-Foot High-Speed Tunnel. NACA RM No. L6J01a, 1946.

4. Jones, Robert T.: Thin Oblique Airfoils at Supersonic Speed. NACA TN No. 1107, 1946.

5. Harmon, Sidney M., and Swanson, Margaret D.: Calculations of the Supersonic Wave Drag of Nonlifting Wings with Arbitrary Sweepback and Aspect Ratio. Wings Swept behind the Mach Lines. NACA RM No. L6K29, 1946.

6. Abbott, Ira H., von Doenhoff, Albert E., and Stivers, Louis S., Jr.: Summary of Airfoil Data. NACA ACR No. L5C05, 1945.

7. Cohen, Doris: Theoretical Distribution of Load over a Swept-Back Wing. NACA ARR, Oct. 1942.

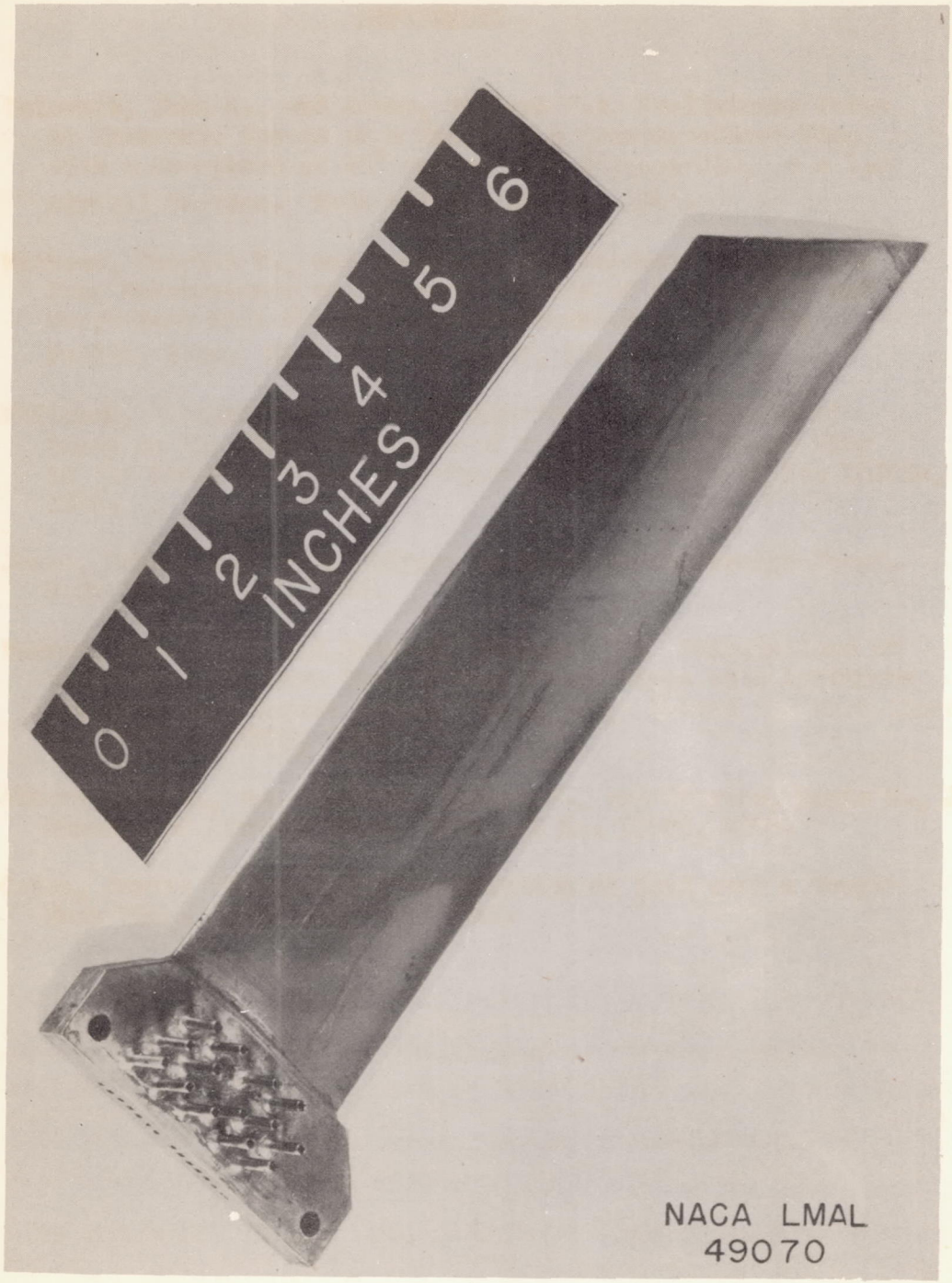

Figure 1.- NACA 65-210 airfoil model.

CONFIDENTIAL

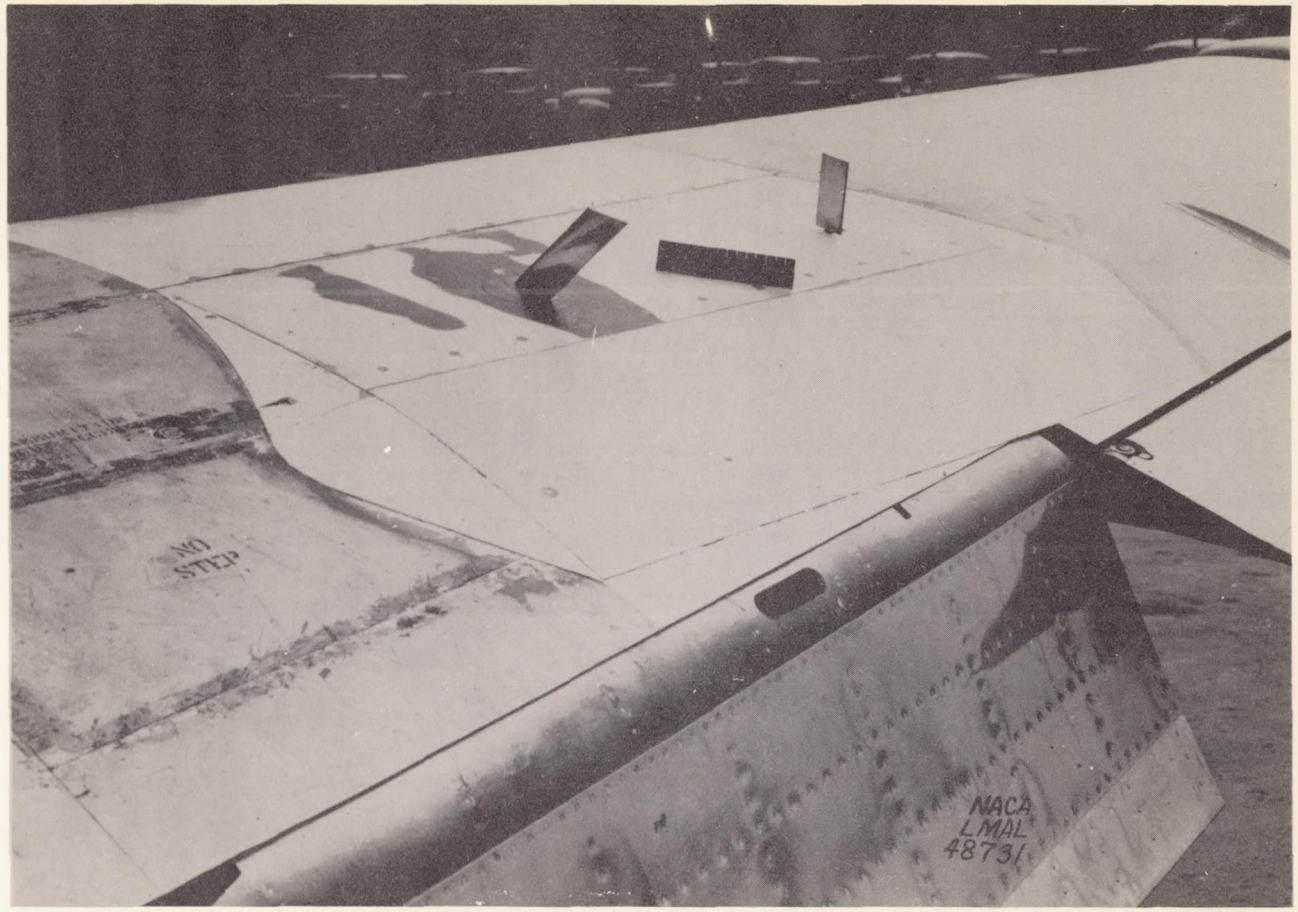

Figure 2.- Airfoil model mounted on airplane wing; orifices at 50 percent semispan, 3.5 aspect ratio.

CONFIDENTIAL

CONFIDENTIAL

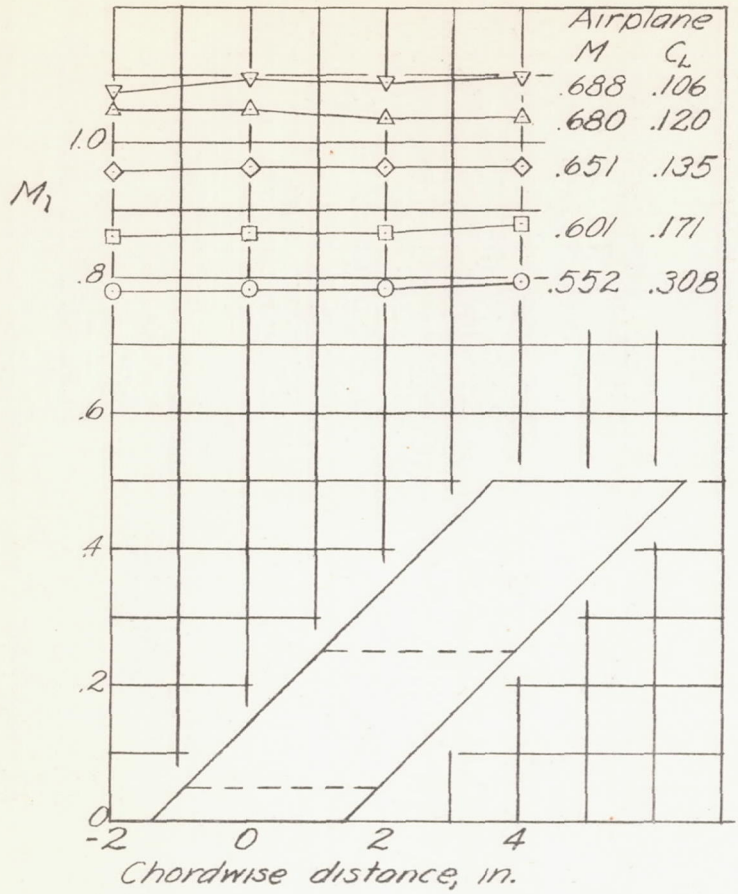

(a). Mach numbers along wing surface.

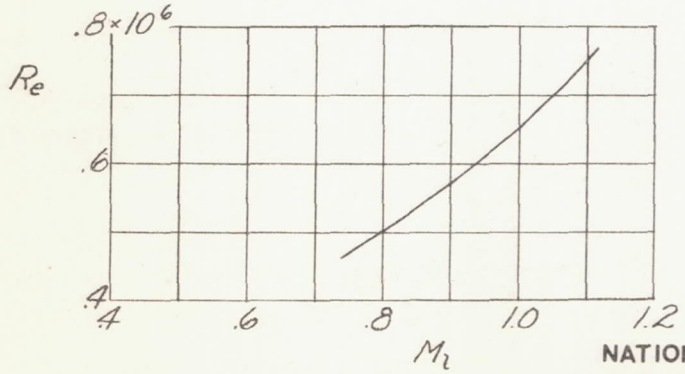

NATIONAL ADVISORY COMMITTEE FOR AERONAUTICS

(b). Reynolds' numbers; 2.83 in. chord.

CONFIDENTIAL

Figure 3.- Typical test conditions.

CONFIDENTIAL

orifice locations

orifice no.	$\frac{x}{c}$	orifice no	$\frac{x}{c}$
1	.03	8	.46
2	.11	9	.51
3	.16	10	.56
4	.21	11	.61
5	.26	12	.66
6	31	13	.71
7	.36	14	.78

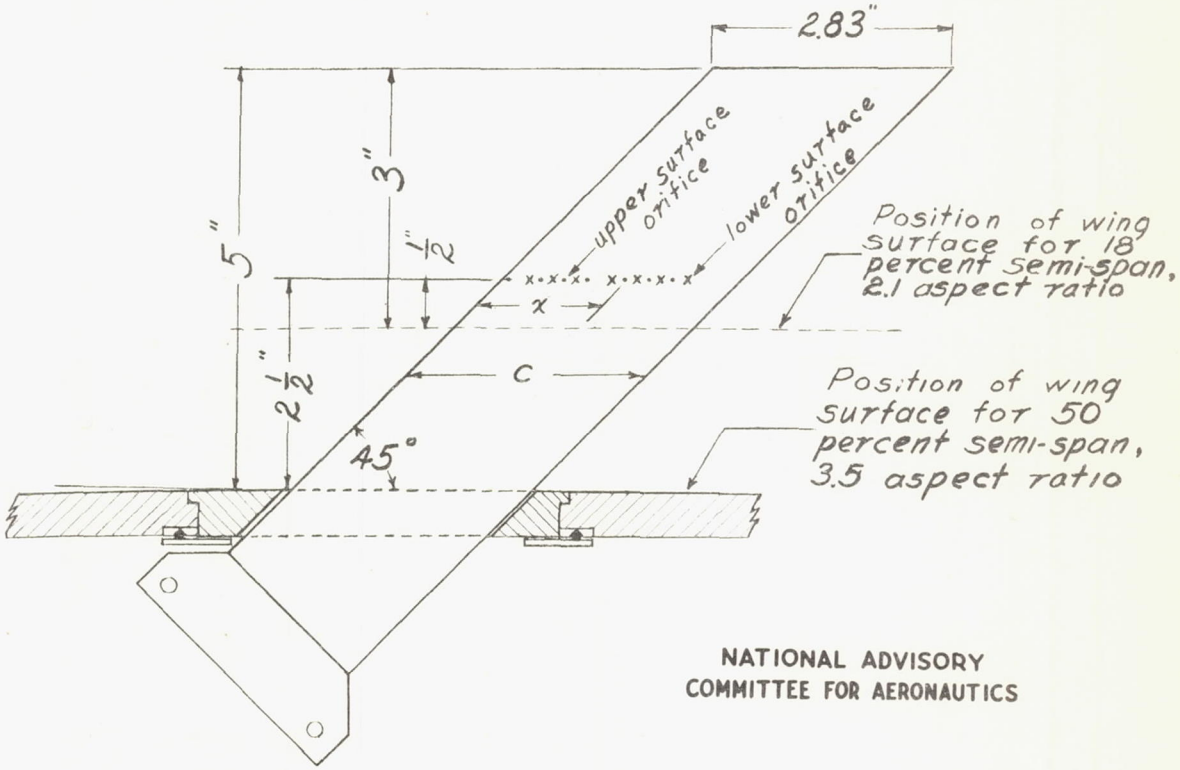

NATIONAL ADVISORY COMMITTEE FOR AERONAUTICS

CONFIDENTIAL

Figure 4.- Sketch of airfoil model in relation to airplane wing.

CONFIDENTIAL

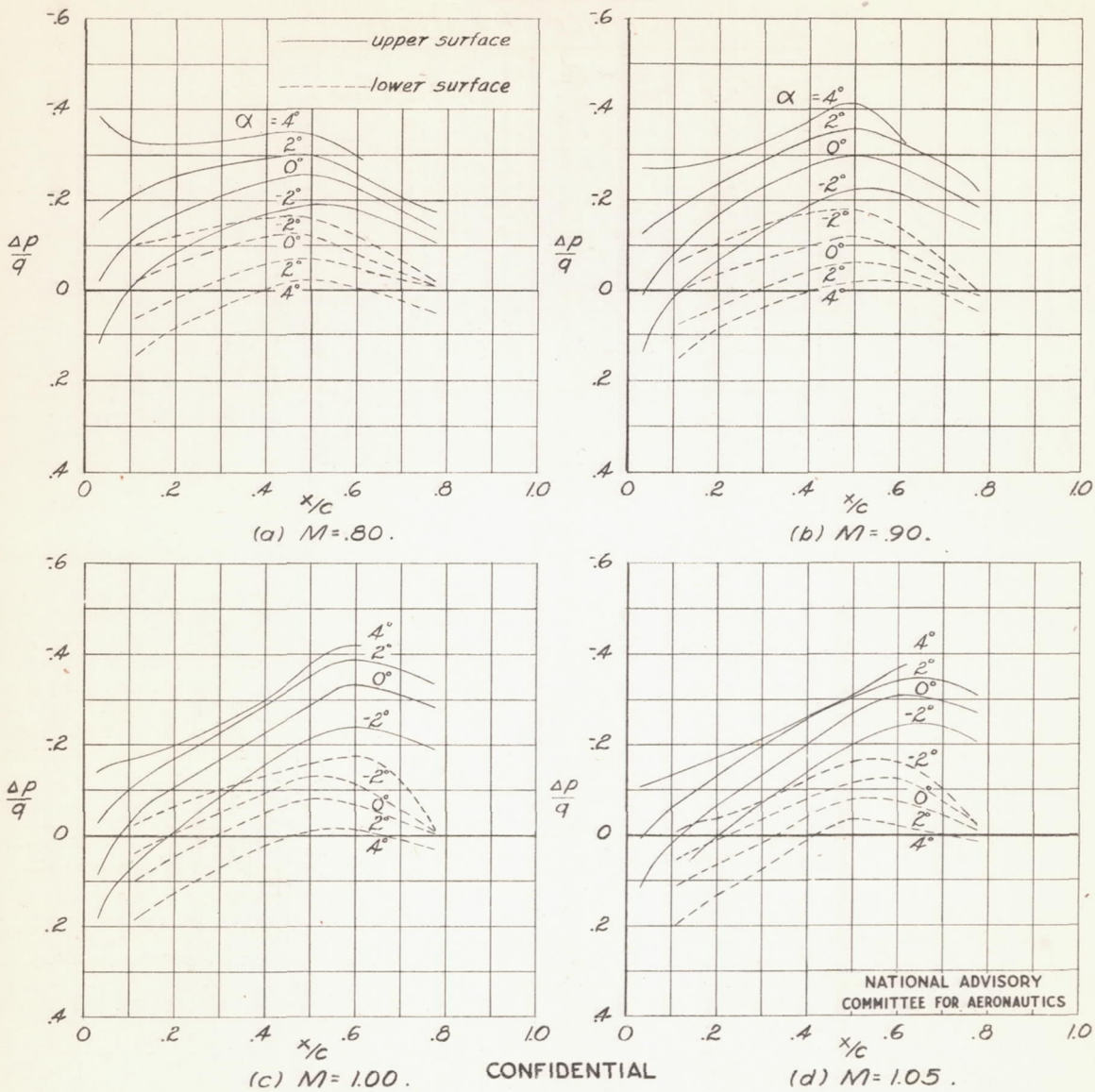

CONFIDENTIAL

Figure 5.- Pressure distributions at 18 percent semispan; $\frac{y}{c_o} = 0.18$, $A = 2.1$.

CONFIDENTIAL

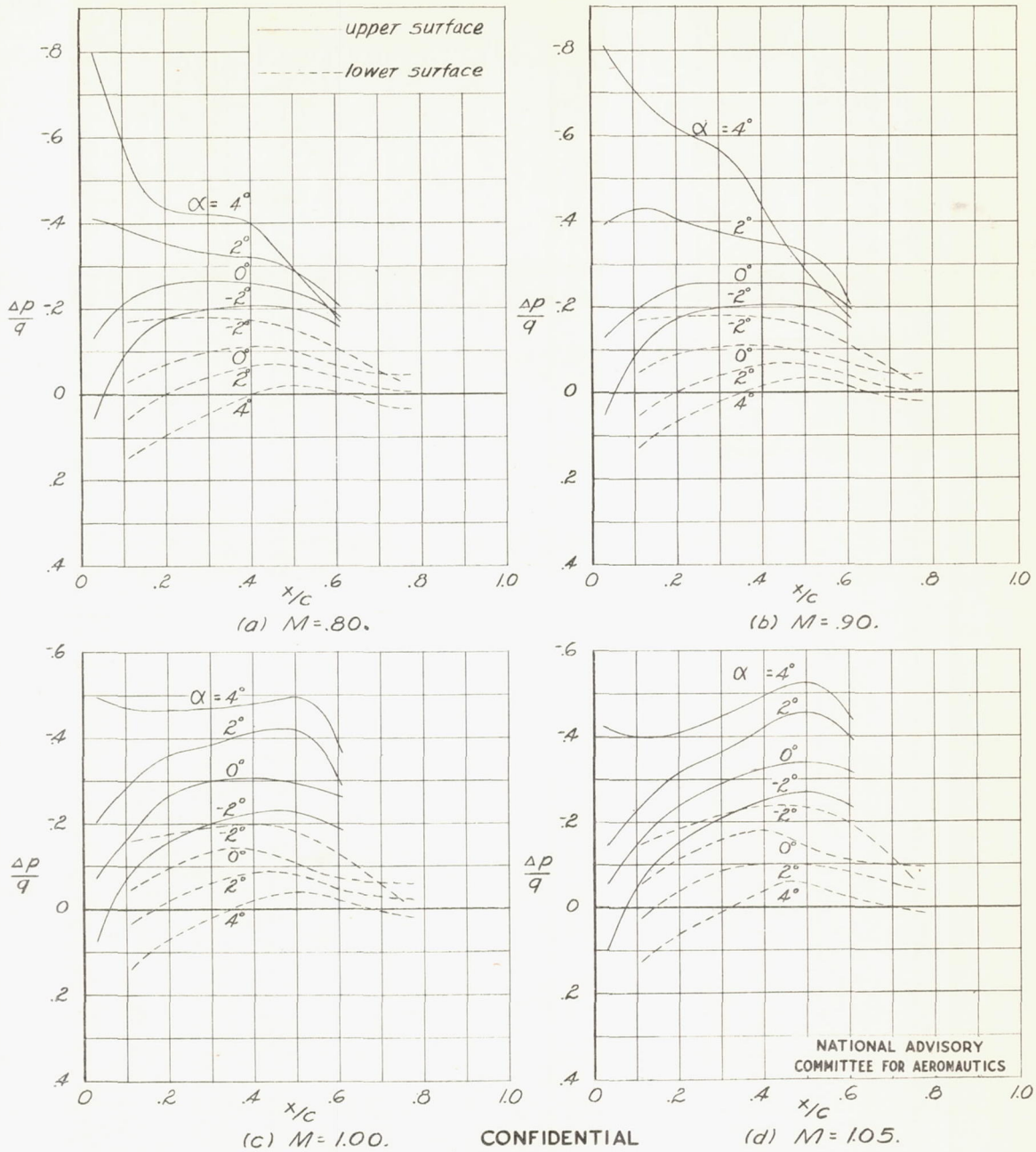

CONFIDENTIAL

Figure 6.- Pressure distributions at 50 percent semispan; $\frac{y}{c_o} = 0.87$, $A = 3.5$.

CONFIDENTIAL

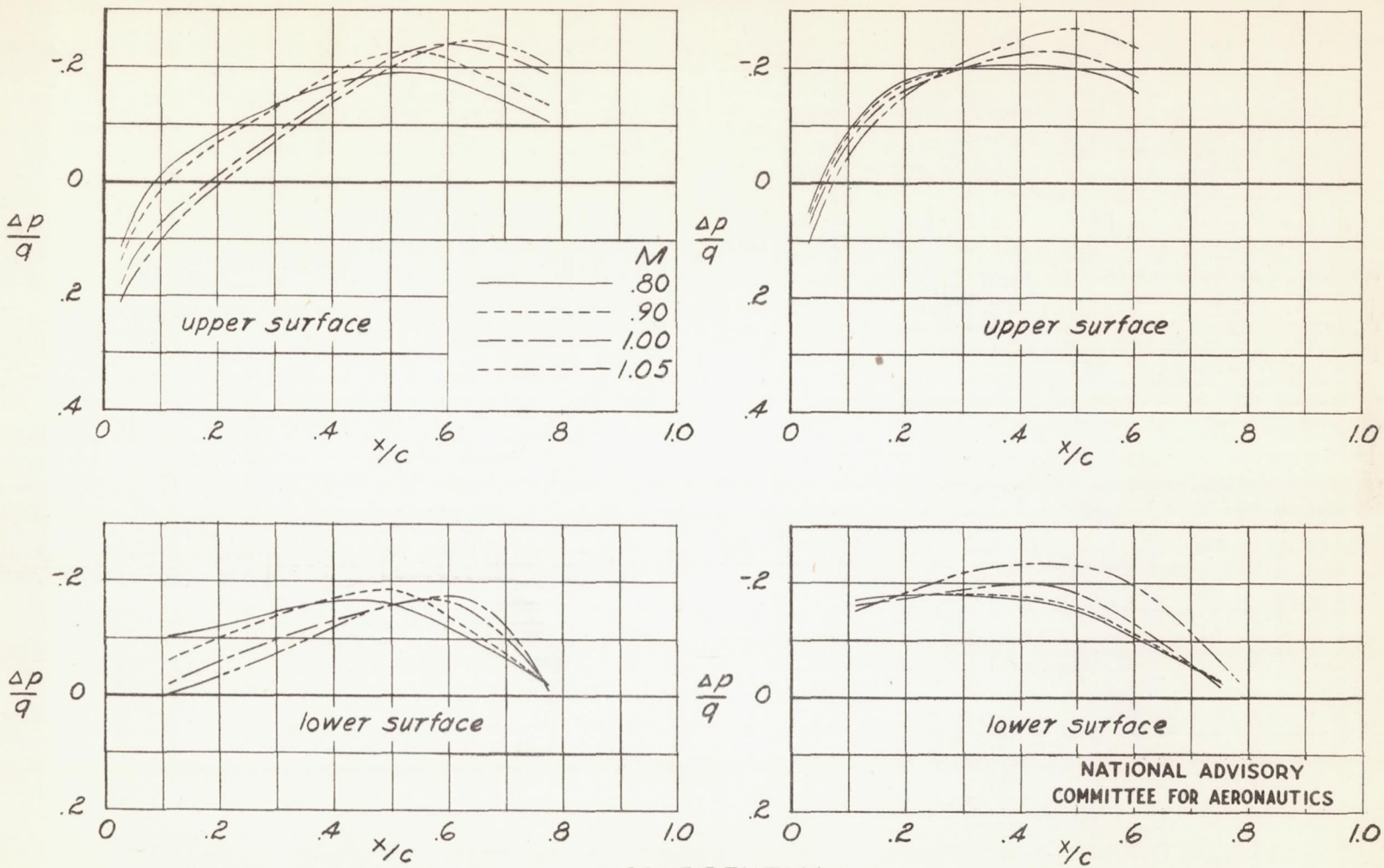

(a) $y = .18\,c_o$, $A = 2.1$. CONFIDENTIAL (b) $y = .87\,c_o$, $A = 3.5$.

Figure 7.- Pressure distributions at $\alpha = -2^{\circ}$ (zero lift).

CONFIDENTIAL

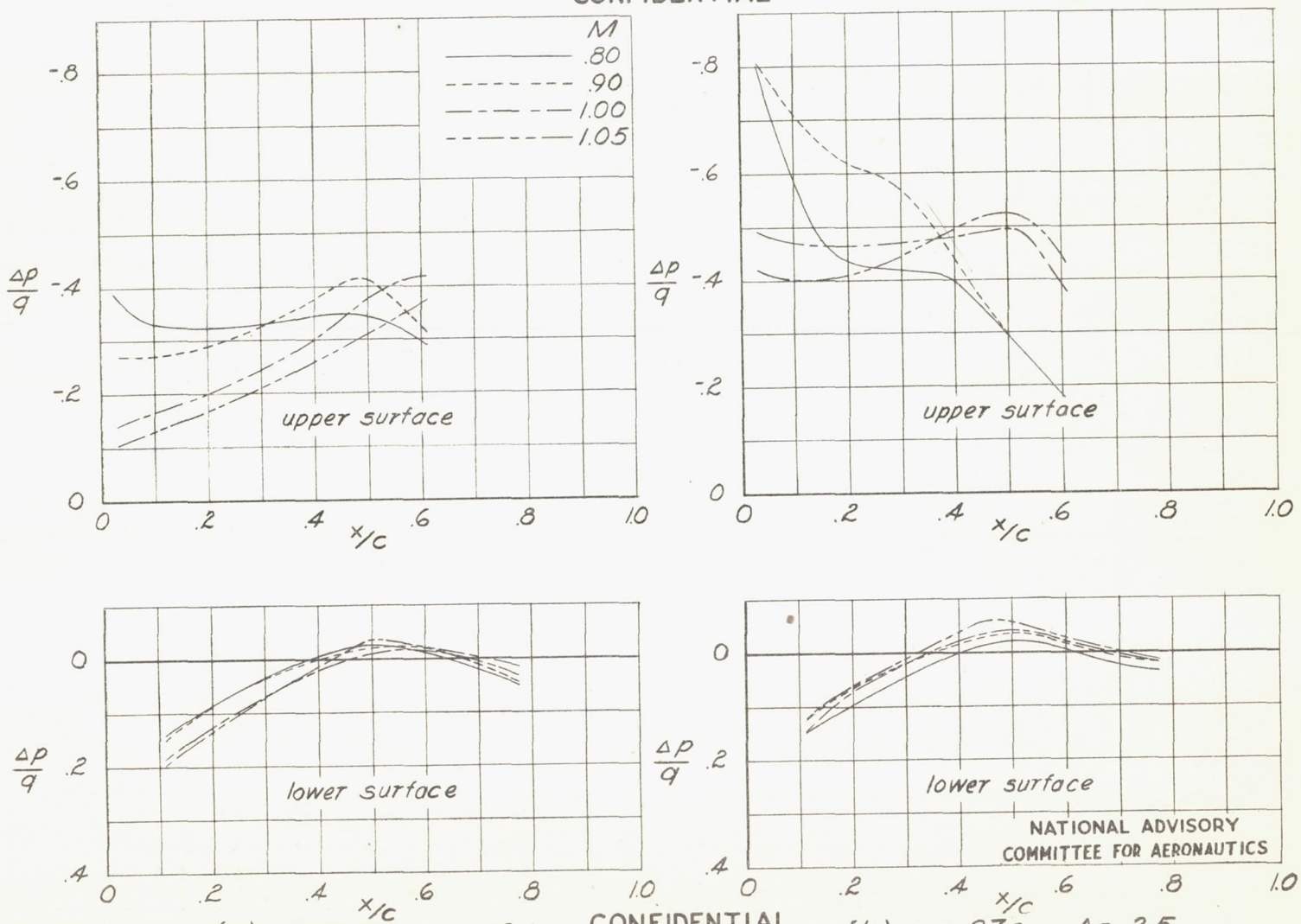

(a) $y = .18\,c_o$, $A = 2.1$. CONFIDENTIAL (b) $y = .87\,c_o$, $A = 3.5$.

Figure 8.- Pressure distributions at $\alpha = 4^{\circ}$.

CONFIDENTIAL

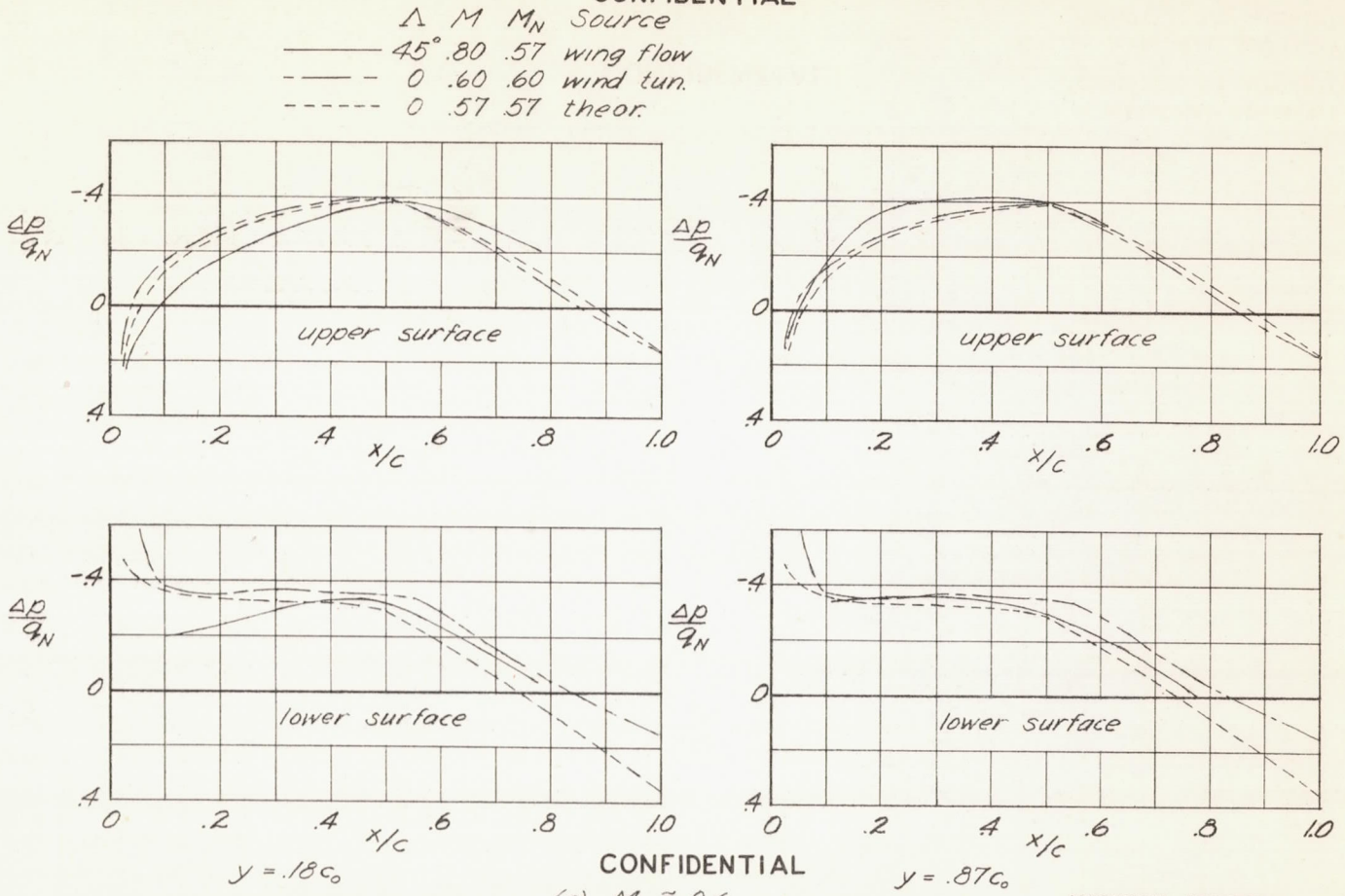

CONFIDENTIAL

(a) $M_N \cong 0.6$

NATIONAL ADVISORY COMMITTEE FOR AERONAUTICS

Figure 9.- Comparison of pressure distributions on swept and unswept wings of NACA 65-210 section at the same normal Mach number and lift coefficient; $c_{l_{N(M=0)}} \cong 0$.

CONFIDENTIAL

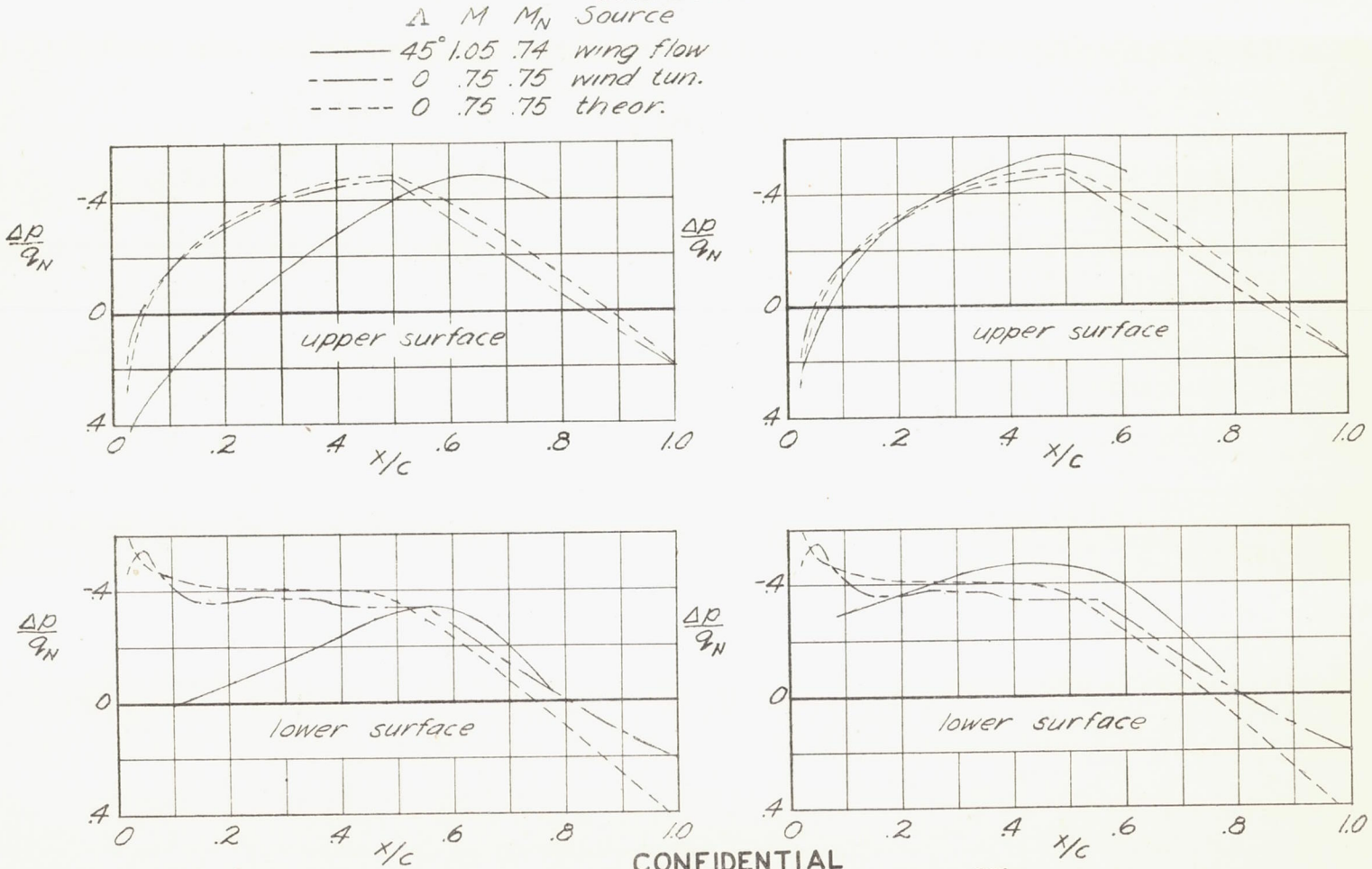

CONFIDENTIAL

(b) $M_N \cong 0.75$

NATIONAL ADVISORY COMMITTEE FOR AERONAUTICS

Figure 9.- Concluded.

CONFIDENTIAL

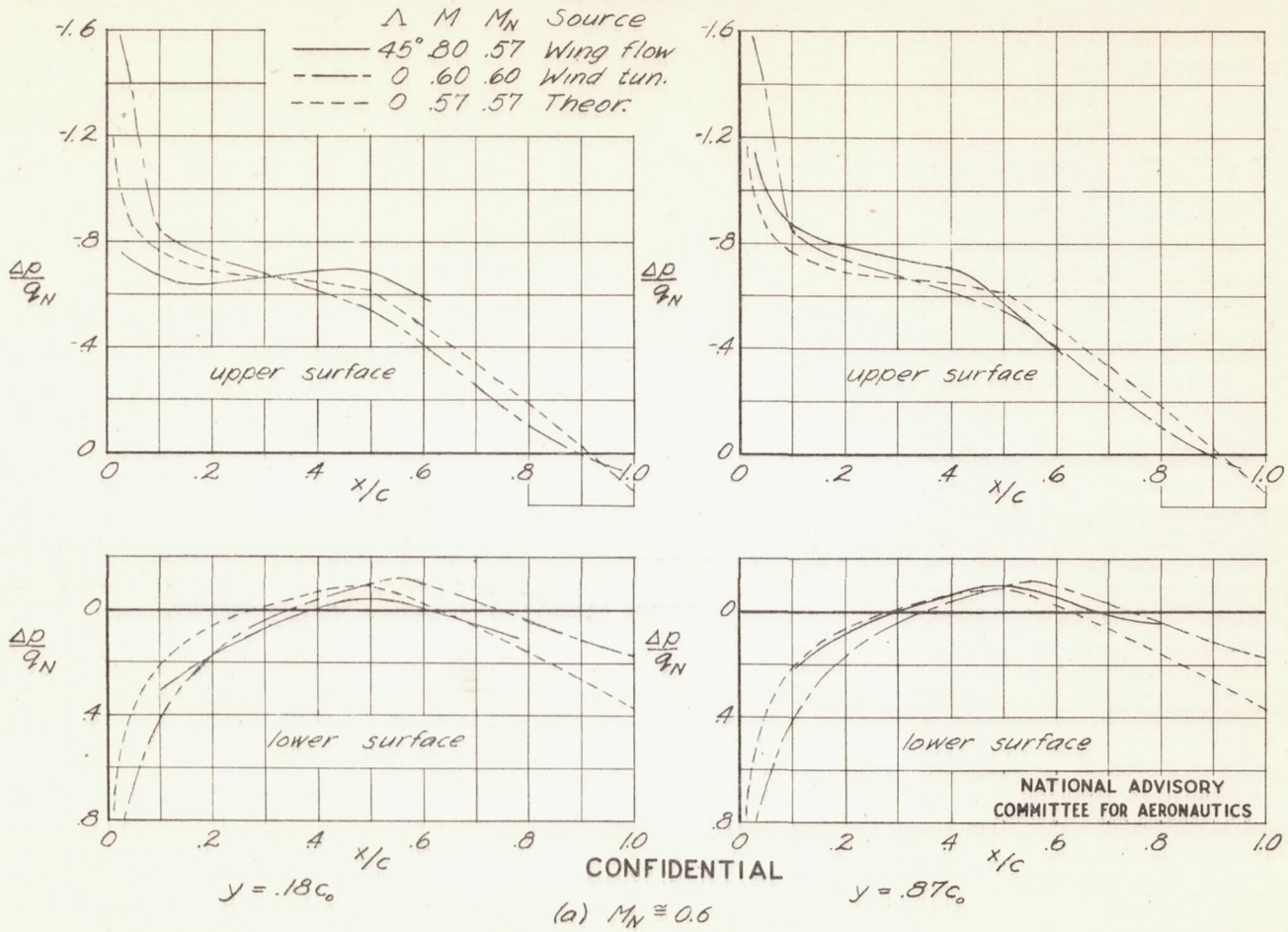

CONFIDENTIAL

(a) $M_N \cong 0.6$

Figure 10.- Comparison of pressure distributions on swept and unswept wings of NACA 65-210 section at the same normal Mach number and lift coefficient; $c_{l_{N(M=0)}} \cong 0.48$.

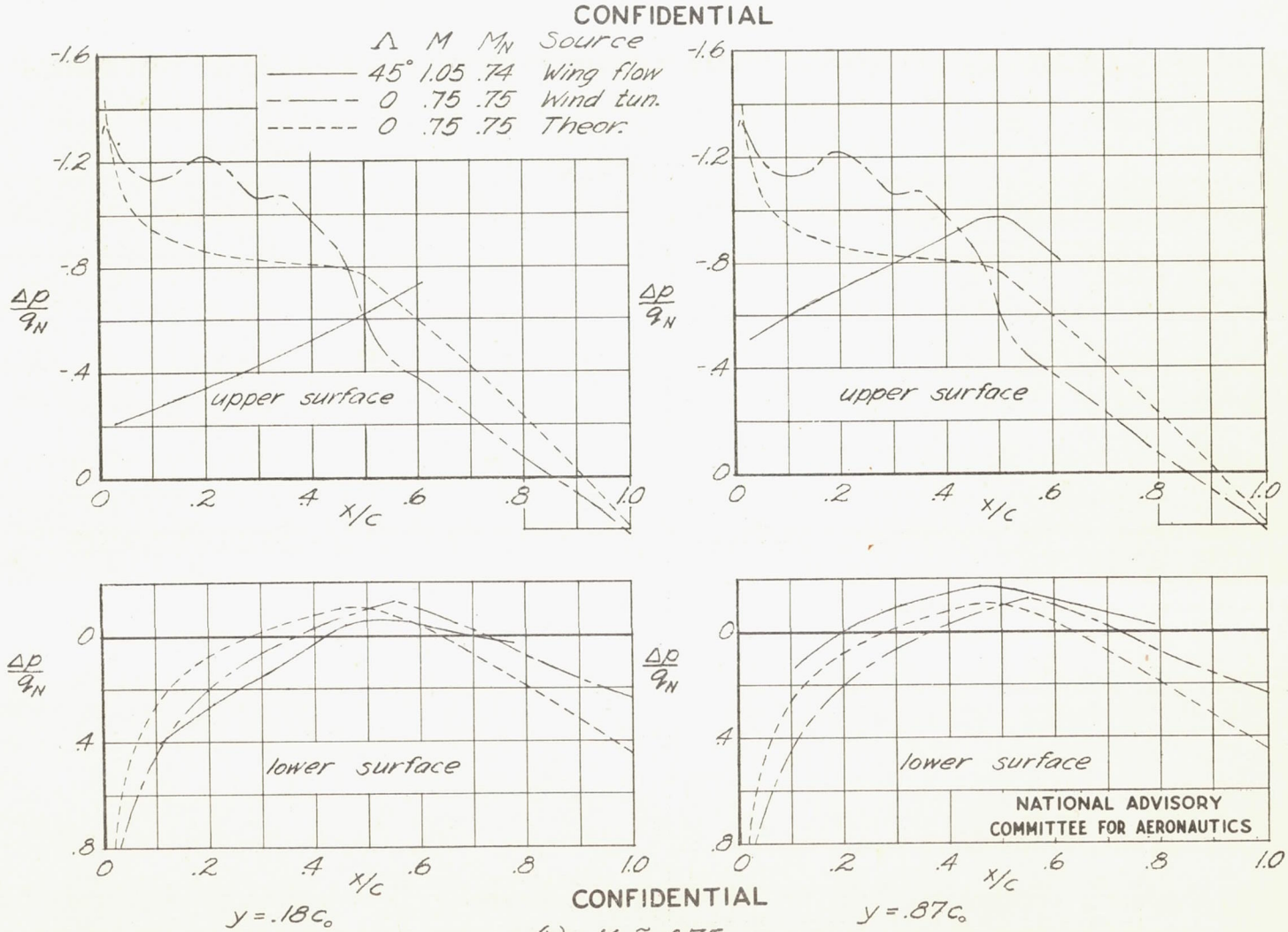

(b) $M_N \cong 0.75$

Figure 10.- Concluded.